

Performance Analysis of Radiation Detection Devices in Elevated Natural Radiation Zones: A Case Study of Mamuju Regency, West Sulawesi Indonesia

Adi Rahmansyah Amir Abdullah¹, Sidik Permana^{1,2,*}, Wahyu Srigutomo², Alan Maulana³, Haryo Seno³, Dikdik Sidik Purnama³, Rasito³, Ismail Humolungo¹, & Zulfahmi¹

¹Doctoral Program in Nuclear Engineering Department, Institut Teknologi Bandung, Jalan Ganesha No. 10, Bandung 40132, Indonesia.

²Physics Department, Bandung Institute of Technology, Jalan Ganesha No. 10, Bandung 40132, Indonesia.

³Indonesia's National Research and Innovation Agency, Jalan Tamansari No. 71, Bandung 40132, Indonesia

*Corresponding author: psidik@itb.ac.id

Abstract

Three radiation detection tools were employed to assess natural radiation levels in Mamuju Regency, West Sulawesi, Indonesia. These tools comprised the NaI(Tl) Scintillator, the Geiger Muller Counter (GMC), and the Electronic Personal Dosimeter (EPD). The NaI(Tl) Scintillator and GMC measured ambient dose equivalent ($H^*(10)$), while the EPD exclusively gauged personal dose equivalent ($Hp(10)$). A total of 75 measuring points were designated for assessment. Results from $H^*(10)$ measurements indicated that the GMC recorded an average $H^*(10)$ 41% higher than that of the NaI(Tl) Scintillator, with specific rates of 0.769 $\mu\text{Sv}/\text{h}$ and 0.457 $\mu\text{Sv}/\text{h}$, respectively. Both instruments exhibited proficiency in detecting elevated levels of radiation. Discrepancies in the outcomes were attributed to differences in detector type and efficiency. The GMC, equipped with an energy-compensated detector, demonstrated enhanced efficiency compared to the NaI(Tl) Scintillator, particularly when subjected to high energy flux radiation. Anomalies emerged in the $Hp(10)$ measurements, which surpassed the $H^*(10)$ measurements. This difference is due to the EPD's use of a conventional GM detector, which is capable of detecting gamma, beta, and X-ray radiation.

Keywords: ambient dose equivalent; electronic personal dosimeter; geiger muller counter; Mamuju; NaI(Tl) scintillator; personal dose equivalent.

Introduction

The importance of radiation detectors becomes evident in the context of radiation detection. These detectors play a pivotal role in accurately measuring and recording radiation levels in specific environments, areas, or regions. They enable the creation of detailed visual representations that depict variations in radiation intensity across a given area or environment. Radiation mapping in environmental radiation monitoring, emphasizing its role in identifying radiation level anomalies, assessing radiation monitoring effectiveness during nuclear or radiological emergencies, detection and localization of nuclear and radioactive materials associated with illicit trafficking, and monitoring gamma radiation levels in critical public locations and identification of Naturally Occurring Radioactive Materials (NORM) concentrations across different contexts (Marques et al., 2021; Saindane et al., 2020).

Radiation detectors operate by detecting changes induced by the absorption of radiant energy within their materials, measuring the energy from radiation generated during decay. These detectors typically fall into three categories: gas-filled detectors, scintillator detectors, and semiconductor detectors. Each type operates differently, offers varying sensitivity levels, and is suited for different purposes. Choosing a detector depends on specific requirements such as sensitivity, energy precision, and the type of radiation to be detected (Alatas et al., 2016; Lehto, 2016; Patel & Mazumdar, 2023). The NaI(Tl) Scintillator Spectrometer and the Gamma Ray HPGe Spectrometer are two primary measurement tools employed for monitoring gamma radiation anomalies. These devices operate based on scintillation principles in radiation detection (IAEA, 2003; Lehto, 2016; Marques et al., 2021). Another commonly used instrument is the Geiger Counter, which operates based on the ionization of radiation with a gas-filled detector.

Despite having distinct working principles, both the Geiger Counter and scintillator-based detectors are commonly referred to as survey meters due to their similar applications in radiation detection and measurement.

In radiation protection, a personal dosimeter is a crucial tool used to measure the radiation dose accumulated by an individual over a designated period. Its primary purpose is to monitor radiation exposure in occupational settings, such as nuclear facilities, medical facilities utilizing radiation, industrial sites, and research laboratories (Izewska & Rajan, 2005).

In this study, we employed three distinct detectors, the NaI(Tl) Scintillator, Geiger Counter, and Electronic Personal Dosimeter, to measure outdoor terrestrial ambient dose equivalent and personal dose equivalent in Mamuju Regency, West Sulawesi, Indonesia. This region is renowned for its elevated natural radiation levels, attributed to areas containing prospective radioactive mineral deposits. Our primary aim was to assess the performance of these detectors in an environment with heightened natural gamma radiation exposure.

The NaI(Tl) Scintillator and Geiger Counter functioned as survey meters, quantifying operational quantities of ambient dose equivalent ($H^*(10)$), while the Electronic Personal Dosimeter (EPD) measured the operational quantity of Personal Dose Equivalent ($Hp(10)$). We delved into the discrepancies in response between the Scintillator and Geiger Muller detectors when measuring $H^*(10)$, alongside examining the Electronic Personal Dosimeter's response in measuring $Hp(10)$.

Research Methods

Materials

Data acquisition involved three instruments, including the handheld Canberra Survey meter Inspector A1000, equipped with IPROS-2 Stabilized 2" x 2" NaI probe, and the other two tools are the handheld Canberra Mini Radiac Geiger Muller equipped with energy compensated GM detector, and Smart Rad Electronic Personal Dosimeter with GM built-in type detector with openable beta window. From now on, the detectors used are referring to NaI(Tl) Scintillator, GMC, and EPD. These three instruments belong to the Environmental Radiation Analysis Laboratory, National Research and Innovation Agency of Indonesia, Bandung, which is commonly used for monitoring radiation around the TRIGA MARK II reactor. They have never been used for monitoring radiation in an environment with a high background of natural radiation. All three instruments have been calibrated at the Safety Technology and Radiation Metrology Laboratory (LTKMR), National Research and Innovation Agency, Indonesia, using the substitution method (IAEA Safety Reports Series No. 16, 2000). The detector was exposed in a standard gamma radiation field of ^{137}Cs (LTKMR, 2022a, 2022b).

The NaI(Tl) Scintillator used is a handheld NaI spectrometer designed to operate in all types of environments (Canberra, 2011). The NaI(Tl) 2" x 2" detector, such as the one employed in this research, has efficiency ranges from 17.49% to 90.56% within the energy range of 143.8 keV to 2.614 MeV, with specific efficiency for natural sources of ^{238}U and ^{232}Th ranging from 17.49% to 64.09% in the energy range of 609.30 keV to 2.614 MeV (Kadum & Dahmani, 2015).

Meanwhile, the Mini Radiac serves as personal radiation-measuring device. This device is equipped with technical specifications including an energy-compensated GM detector with application for gamma detection only. Further detailed detector specifications are available (Mirion, 2018). It ensures accuracy within $\pm 30\%$ of 100 $\mu R/h$ (1 $\mu Sv/h$) to 200 R/h (2.0 Sv/h), with an efficiency of $\pm 40\%$ within the energy range of 60 keV to 1.5 MeV. The optimization of wrapping for this survey meter detector (Zhu et al., 2006) and the analysis of the technical data for this detector type reveals that higher count rates correspond to elevated dose rate readings (NUSTL, 2016).

The EPD is a handheld and compact device designed to measure and pulse beta, X-ray, and gamma radiation. This device is used to measure personal dose equivalent ($Hp(10)$) with the type of detector used is a conventional GM (Geiger-Müller) detector that is not energy-compensated, meaning it has higher efficiency at low energy levels (Enviro, n.d.).

To validate the ambient data from survey meter and EPD, 21 soil samples were collected from the site and subjected to laboratory testing using the XRF method at the Radiation Laboratory, National Research and Innovation Agency of Indonesia (BRIN), in Yogyakarta and the Coaxial HPGe Gamma Spectrometer at the Environmental Radiation

Laboratory, National Research and Innovation Agency of Indonesia (BRIN), in Bandung. Each sample weighed between 3 to 5 kg and was stored in polythene plastic.

Because the research location was on a different island and far from the laboratory where the samples would be tested, they were first dried in sunlight for 3-5 days (depending on the weather) to reduce their water content and lower shipping costs. The transport of the samples from the research location to the laboratory took approximately 14 days, involving both land and sea travel.

Once they arrived at the laboratory, the samples were then heated in an oven at 100 °C for 24 hours, crushed with a grinder, and sieved to a size of 100 mesh using a sieve shaker. The sieved samples were then stored in 500 g Marinelli plastic containers, sealed, and left to stand for one month before being measured with the HPGe Gamma Spectrometer to calculate their radionuclide activity.

Study Area

The research was conducted in Mamuju Regency, the capital of West Sulawesi Province, Indonesia, as shown in Figure 1. The primary area of this research is on areas displaying indications of radioactive mineral deposits (Sukadana et al., 2021; Syaeful et al., 2014) and encompasses villages surrounding the radioactive mineral deposit area.

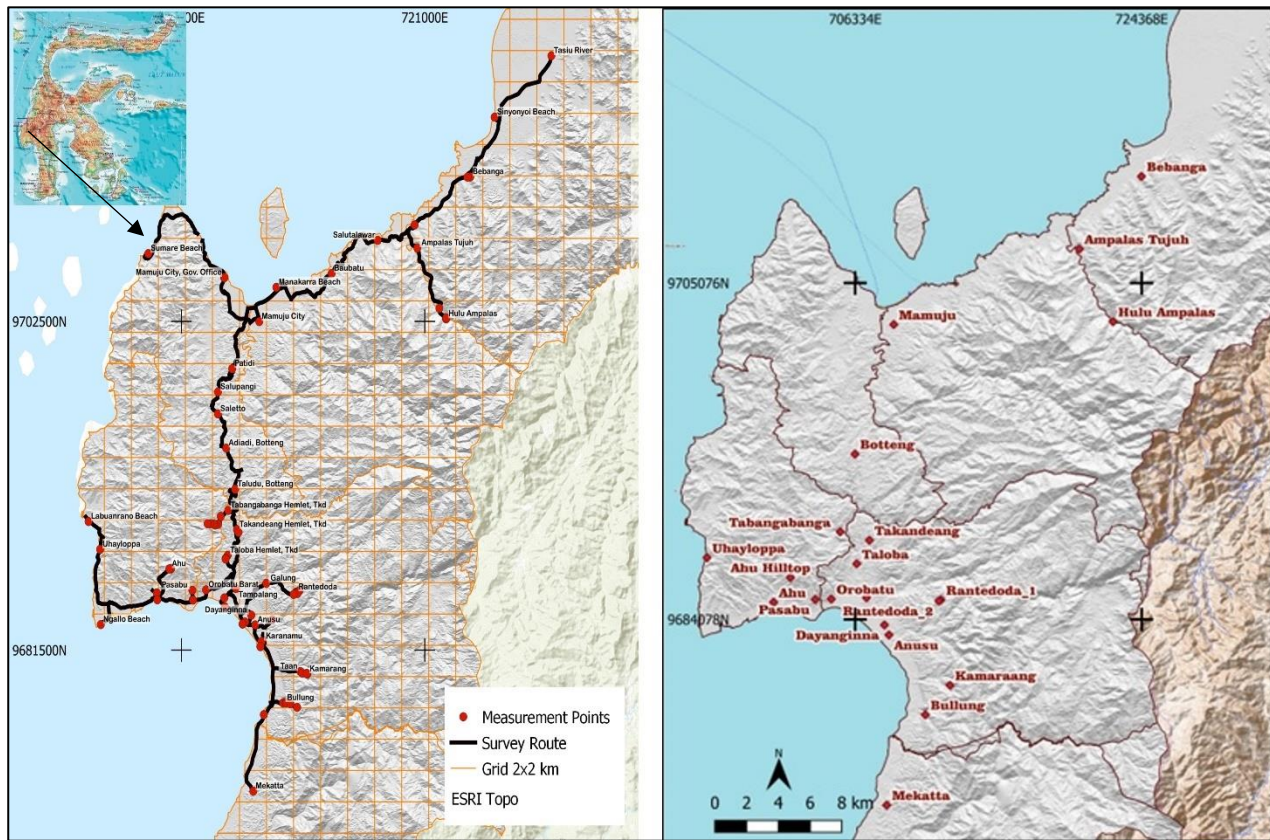


Figure 1 Research location in Mamuju Regency, West Sulawesi, Indonesia. The ambient dose measurement point (right) and the soil samples sampling location (left).

Geologically, the rocks in Mamuju Regency consist predominantly of volcanic rocks, specifically categorized under the Adang volcanic rock unit. The mineralization of radioactive elements, leading to elevated radiation dose rates, has been pinpointed in the Adang, Ampalas, Tapalang, and Malunda volcanic complexes (Sukadana et al., 2015). The presence of uranium and thorium deposits is influenced by various factors, including lithology, geological structure, and hydrothermal fluids, all of which play pivotal roles in determining the radioactivity levels in the region. High uranium and thorium concentrations are recorded in weathered volcanic rocks in this area. The primary radioactive minerals found include thorianite and davidite, accompanied by secondary minerals such as gummite and autunite (Sukadana et al., 2016). Secondary enrichment occurs over time through the weathering process where the tropical

climate strongly supports the formation of soil containing highly radioactive elements, this process is called supergene enrichment (Syaeful et al., 2014).

The predominant soil type in Mamuju Regency is laterite. It is a reddish or brown residual soil that forms in regions with moist tropical and subtropical climates, characterized by good drainage. This type of soil results from chemical weathering near the surface and originates from parent rocks with a high iron (Fe) content, distributed in Mamuju and Mamasa districts (western Sulawesi) are derived by tropical weathering with the rainwater pH ~ 6.5 (the current pH condition) (Godang et al., 2019).

Data Acquisition Method

The morphology of the research area includes hills, valleys, and plains, resulting in a diverse array of data collection locations (Indrastomo et al., 2015). These locations include hilly areas, gardens, forests, riverbanks, beaches, unpaved roadsides, courtyards, and one location within a park. Consequently, the car-borne method was not chosen for data acquisition. Instead, a foot-based survey approach was implemented. This method involves establishing a $2 \times 2 \text{ km}^2$ grid, allowing data recording at any point within each grid and simplifying representation with a single measuring point for each grid. All measurements were conducted outdoors, with measurement points selected at various locations within the grid.

Travel to the measuring points was conducted on foot if they were distant from the main road. If a measuring point was situated alongside an unpaved road, a vehicle was used to reach it. To reach the targeted point, a vehicle was used to get as close as possible, followed by continued travel on foot. The types of surfaces where data were collected varied, with soil being the dominant surface type, followed by sand, unpaved roads, landfill areas, and one location on concrete.

The dose rate data were recorded from a distance of 1 meter above the ground for the NaI(Tl) Scintillator and GMC instrument and the EPD was placed on the team member's chest. The radiometry map is used as a guide to determine the measurement points (Sukadana et al., 2021). At each point, coordinates were captured using the Garmin e-Trex 10 portable GPS. Data recording followed an on-and-off pattern, with data being recorded at each designated point before moving on to the next grid. The EPD device was kept on constantly from the start to the end of data collection to track the total radiation exposure or cumulative dose.

Before delving into the disparities in response between the GMC and NaI(Tl) scintillator in recording the ambient dose equivalent ($H^*(10)$), it is crucial to understand the factors contributing to the elevated radiation levels in the soil. In this study, data on the concentration and activity of radionuclides were obtained through both XRF and HPGe Gamma Spectrometry tests.

Data Analysis Method

The data collected during the recording process with the three instruments include ambient dose equivalent ($H^*(10)$), measured by NaI(Tl) Scintillator and GMC, and personal dose equivalent ($H_p(10)$) by EPD, both measuring dose rates in $\mu\text{Sv}/\text{h}$.

Statistical methods are used to analyze data from each tool. The Shapiro-Wilk test is applied to determine whether the data distribution is normal. If the data is normally distributed, the p-value is calculated using the ANOVA method to assess the differences in output data between the tools. If the data is not normally distributed, the p-value is calculated using a non-parametric statistical method, specifically the Kruskal-Wallis ANOVA. The analysis is conducted at a confidence level of 0.05. A multivariate statistical analysis was performed using Principal Component Analysis (PCA) to explore the relationships between measurement variables from the survey tools and laboratory tests on soil samples, which were conducted using the XRF and HPGe Gamma Spectrometer methods. All the statistical analyses were performed with the assistance of OriginLab student version software.

Since direct calibration in the field was not conducted in this research, a crucial step in analyzing the differences in performance among the tools is to understand the characteristics of each detector. Information about each detector type, including its energy range and efficiency, is essential for interpreting the tools' responses to the high levels of

natural radiation exposure. Therefore, a literature review was conducted on the properties of each detector, along with studies related to the performance of gamma detectors under high radiation exposure.

Result and Discussion

The Data

We collected 75 sets of data from environmental radiation measurements using a NaI(Tl) Scintillator, GMC, and EPD. The descriptive statistical analysis revealed that the mean, standard deviation, and standard error for all the measurement points are presented in Table 1. The Shapiro-Wilk test indicates that the obtained data is not normally distributed. Therefore, the Spearman correlation is used to analyze the correlation between variables (Heryana, 2023). The data correlation coefficient between the measurements of the NaI(Tl) Scintillator and the GMC is 0.93, between the NaI(Tl) Scintillator and the EPD is 0.7, and between the GMC and the EPD is 0.76.

Since the data were not normally distributed, the p-value was evaluated using the Kruskal-Wallis ANOVA at a confidence level of 0.05. It was found that the p-value between the NaI(Tl) data and the GMC and EPD data was <0.0001, indicating a significant difference. Meanwhile, the p-value between the GMC and EPD data was 1, indicating no significant difference. This may be related to the differences in the working principles of the three instruments. NaI(Tl) operates on the principle of scintillation, while GMC and EPD use gas ionization

The analysis of environmental radiation exposure ($H^*(10)$) is on comparing the data of the NaI(Tl) Scintillator with the GMC. Meanwhile, EPD data cannot be compared with the NaI(Tl) Scintillator and GMC data due to differences in their working principles. EPD measures $H_p(10)$, which depends on the angle of incidence, while the survey meter does not.

Table 1 The average, standard deviation, and median values of the recorded data.

	NaI(Tl) Scintillator nSv/h	GMC nSv/h	EPD nSv/h
N total	75	75	75
Mean	454	768	985
Standard Deviation	316	452	822
Geometric Mean	341	643	746
Geometric SD	2.35	1.86	2.10
Minimum	21	108	159
Median	399	742	673
Maximum	1606	2376	4410

The distribution of radiation dose rate values measured by the three instruments is depicted in Figure 2. All instruments recorded high dose rate values, with the EPD values exceeding those measured by the other two instruments exceeding the global average absorbed dose rate for gamma radiation, that is 59 nGy/h (equivalent to 59 nSv/h) (Tzortzis & Tsertos, 2004; UNSCEAR, 2000).

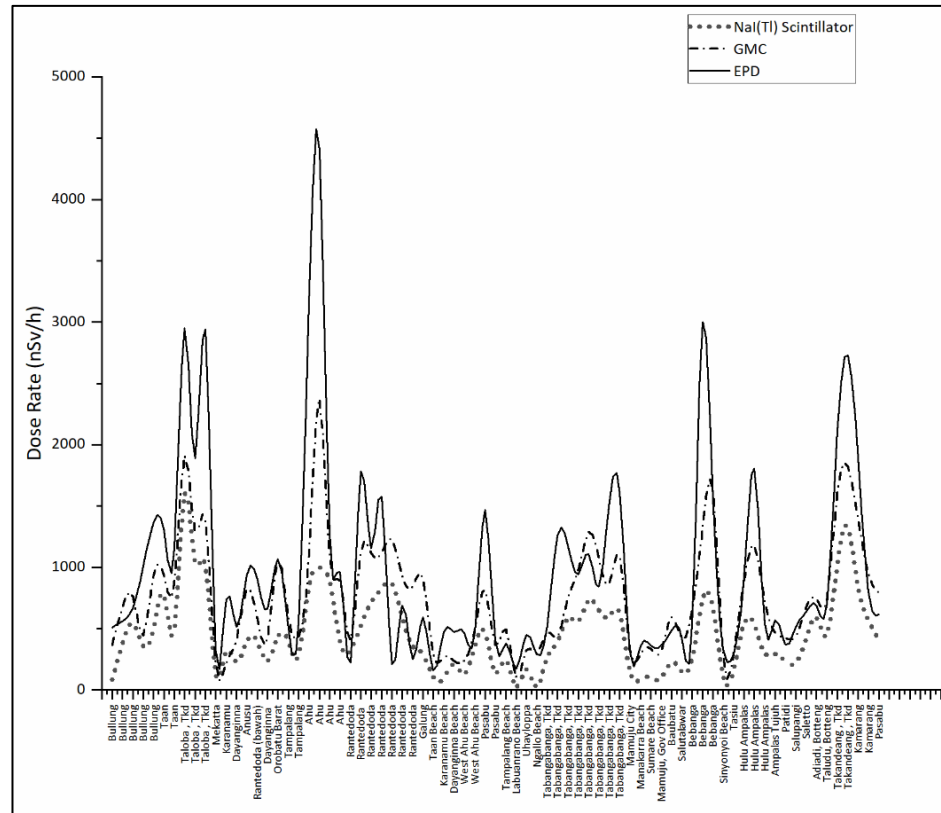


Figure 2 The distribution of radiation dose rate measurements from all measurement points was gathered using various radiation monitoring devices. These include EPD (solid line), GMC (dashed line), and NaI(Tl) Scintillator (dotted line).

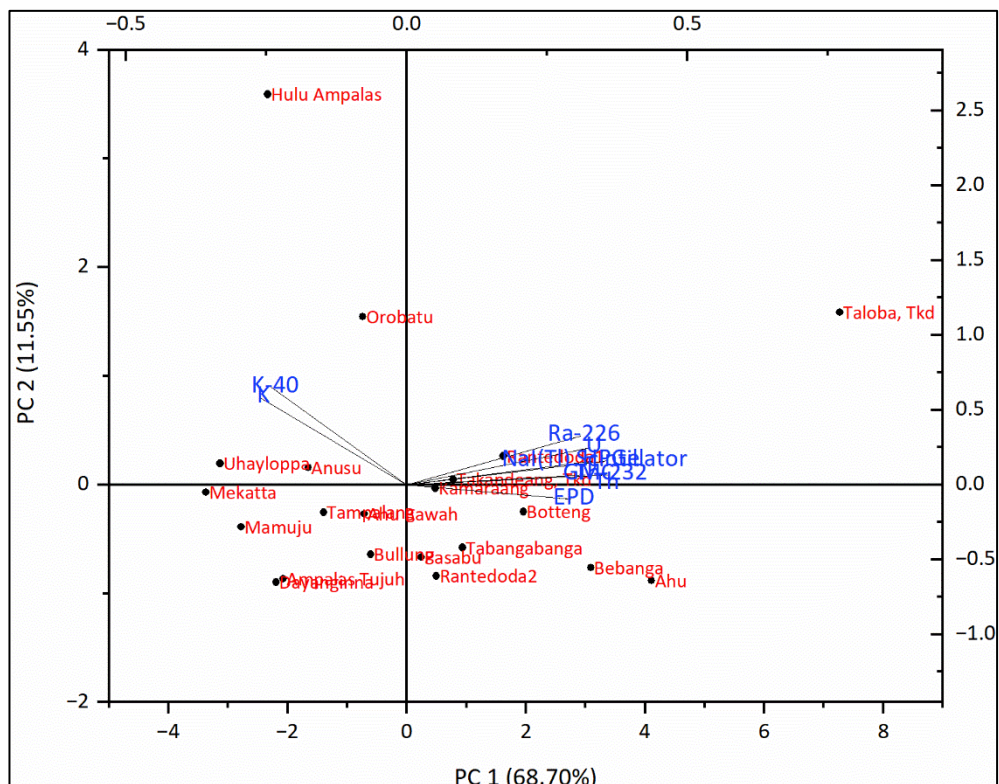


Figure 3 A biplot graph of multivariable correlations using the principal component analysis (PCA) method. This graph displays the relationships among the linear combinations of data for radiation dose rate, absorbed dose, and radioactivity of radionuclides ^{226}Ra , ^{232}Th , and ^{40}K , as well as the concentration of U, Th, and K.

Table 2 The XRF and HPGe Gamma Spectrometry data from 21 soil samples.

Location	Concentration			Activity (Bq/kg)		
	Th (ppm)	U (ppm)	K (%)	^{226}Ra	^{232}Th	^{40}K
Ahu Hill	2,610	295	0.04	966	2591	139
Pasabu	1,390	205	1.26	651	1688	490
Takandeang	716	219	3.88	635	740	355
Taloba	3,520	578	0.15	2553	4402	276
Tabangabanga	782	239	1.73	873	1983	170
Rantedoda1	2,430	367	1.70	656	2445	538
Rantedoda2	2,090	314	1.86	266	1208	280
Kamarang	890	320	2.50	784	846	482
Bebanga	2,010	467	0.14	646	2979	187
Hulu Ampalas	474	319	8.90	555	767	1793
Botteng	1,620	475	0.19	1434	2119	197
Ampalas Tujuh	313	86	4.00	402	628	245
Ahu	835	214	1.92	525	1206	724
Orobatu	981	188	4.11	1026	1221	1272
Tampalang	633	173	2.11	536	883	770
Dayanginna	657	88	2.56	212	545	613
Anusu	661	156	2.06	606	1059	960
Bullung	1,110	115	2.08	164	1250	632
Mekatta	139	43	4.75	220	263	848
Uhayloppa	248	48	4.33	195	478	1064
Mamuju City	489	54	2.74	201	551	961

The XRF data reveals that the average concentrations of U, Th, and K in the 21 soil samples are significantly higher than the global average concentrations of U, Th, and K in surface soil, which are 2.8 ppm for U, 2.4 ppm for Th, and 1.3 ppm for K (Tzortzis & Tsertos, 2004; UNSCEAR, 2000).

In Figure 3, the principal component analysis of the variables for radiation dose rates measured directly with a survey meter and absorbed dose data measured using the HPGe method, along with their linear combination with the activities of radionuclides ^{226}Ra , ^{232}Th , and ^{40}K , as well as the concentrations of U, Th, and K measured using the XRF method, is shown.

The PC-1 and PC-2 axes explain that 68.70% of the variable spread is dominated by the activities of ^{226}Ra and ^{232}Th measured by the survey meter and HPGe spectrometer, supported by the concentration data of U and Th, which are dominant on the PC-1 axis. Meanwhile, the activity of ^{40}K and the concentration of K are evenly distributed on the PC-2 axis, accounting for 11.55%. The dose rate and absorbed dose components form a strong correlation with the activities of radionuclides ^{226}Ra and ^{232}Th as well as the concentrations of U and Th, with the variables clustering around the PC-1 axis.

The activity of ^{232}Th appears more dominant, reinforced by the Th concentration variable, whose axis aligns exactly with the positive PC-1 axis. In contrast, the activity of ^{40}K and the concentration of K are balanced between the negative PC-1 axis and the positive PC-2 axis. In principal component analysis (PCA), long vector positions indicate a strong influence on the principal component axes, PC-1 and PC-2. In this case, soil samples from Taloba hamlet (Takandeang village) show the highest activities of radionuclides ^{226}Ra and ^{232}Th as well as the concentrations of U and Th, while samples from Orobatu and Hulu Ampalas villages show the highest activity of ^{40}K and K concentrations. Soil samples from Takandeang hamlet (Takandeang village), Kamarang, Botteng, and Rantedoda_1 villages have more dominant U and Th contents with low K concentrations. Meanwhile, soil samples from Pasabu, Bebunga, Rantedoda_2, and Ahu villages have high U and Th contents but also high K concentrations. The Rantedoda 1 and 2 villages show differences in K content despite close sampling points, possibly due to K leaching during weathering processes as K is one of the immobile elements in geochemistry.

The villages of Takandeang, Ahu, Bebunga, Botteng, Pasabu, and Hulu Ampalas are categorized as potential areas for radioactive mineral deposits (Sukadana et al., 2021; Syaeful et al., 2014). Meanwhile, Soil samples from Uhayloppa, Anusu, Mekatta, Tampalang, Dayanginna, Ampalas Tujuh, and Mamuju City show low radiation activities and lower

concentrations of radioactive elements, indicating that these areas are not potential regions for radioactive mineral deposits.

Measurement of H*(10) and Hp(10)

The differences in the operation and specifications of devices, such as their response to radiation and types of radiation sources, will result in variations in the measured data values. In this case, the measured H*(10) data difference between the two instruments, NaI(Tl) Scintillator and GMC, is calculated to be 41%, where the GMC readout overestimates the NaI(Tl) Scintillator. This significant difference in readings between the two devices can be attributed to several factors, including the devices' specifications and the very high radiation exposure in the research area. As previously explained, both devices underwent a calibration process using the IAEA standard method at the Radiation Safety and Metrology Technology Laboratory of the National Research and Innovation Agency, ensuring they are ready for use. However, differences in their operation and specifications can contribute to variations in the readings.

The location of the research is also a differentiating factor. Currently, Mamuju Regency is recognized as the area with the highest natural radiation levels in Indonesia (Hosoda et al., 2021; Nugraha, Hosoda, Kusdiana, et al., 2021; Nugraha, Hosoda, Tamakuma, et al., 2021) which has an anomalous area of radionuclide activity in rocks that far exceeds the world average, specifically $22,882 \pm 1602$ Bq/kg for ^{238}U , $33,459 \pm 2348$ Bq/kg for ^{232}Th , and 1909 ± 134 Bq/kg for ^{40}K . and it has been confirmed that the source is natural, with no indication of fallout from other sources (Rosianna et al., 2020).

The differences are visible from the 2D map generated from the QGIS application's dose-rate data, as shown in Figure 5. The disparities in gamma radiation response between the two instruments are also evident. The GMC exhibits higher readings compared to the NaI(Tl) Scintillator, as evidenced by the visibly higher points of radiation intensity in the map generated from GMC data. The highlighted area signifies the variance in response to gamma radiation exposure. The red color, denoting elevated radiation levels, is more accentuated in the GMC data compared to the NaI(Tl) Scintillator. The circled area indicates a difference in the response of the devices to gamma radiation exposure, with GMC marking the areas with higher gamma radiation exposure. This difference can be attributed to factors such as the energy response, radiation type, detector efficiency, calibration, etc. In this case, the H*(10) data measured by the GMC overestimates compared to the NaI(Tl) Scintillator. The efficiency of the NaI(Tl) Scintillator detector typically exhibits a high characteristic at low energies that decreases at higher energies (ALMisned et al., 2022; R Casanovas et al., 2012; Kadum & Dahmani, 2015; Kim et al., 2019; Mouhti et al., 2018; Ramadhan & Abdullah, 2018; Yavuzkanat et al., 2019, 2022).

In contrast, the efficiency of the energy-compensated GM detector increases with increasing photon energy (Kržanović et al., 2019). One possible reason could be that the GM detector in the GMC has a wider measurement range for H*(10) compared to the NaI(Tl) scintillator detector (Canberra, 2011; Kadum & Dahmani, 2015). That means GMC can measure gamma radiation at higher energies where NaI(Tl) Scintillator decreases its efficiency at higher energies. The Geiger-Muller (GM) detector exhibits a greater response to energies above ^{137}Cs (662 keV) compared to a scintillator (Ramon Casanovas et al., 2016). In this case, an overestimate of +40% is expected for 1.5 MeV gamma rays (Canberra, 2011). While the 2" x 2" NaI(Tl) scintillator detector used in this research has a broader energy measurement range, its efficiency is low for high-energy radiation or in situations of high gamma-ray flux exposure (Kadum & Dahmani, 2015; Tavakoli-Anbaran et al., 2009; Yavuzkanat et al., 2019).

Another factor is that scintillator detectors can experience saturation when exposed to high-flux gamma radiation. These phenomena can impact the accuracy of dose rate readings, as the detector may not be able to process all incoming radiation events effectively, leading to an underestimation or overestimation of the actual radiation levels. Saturation occurs when the scintillator's response becomes overwhelmed by high-energy radiation, reaching a maximum response level and thus underestimating the true radiation level (Lecoq, 2020).

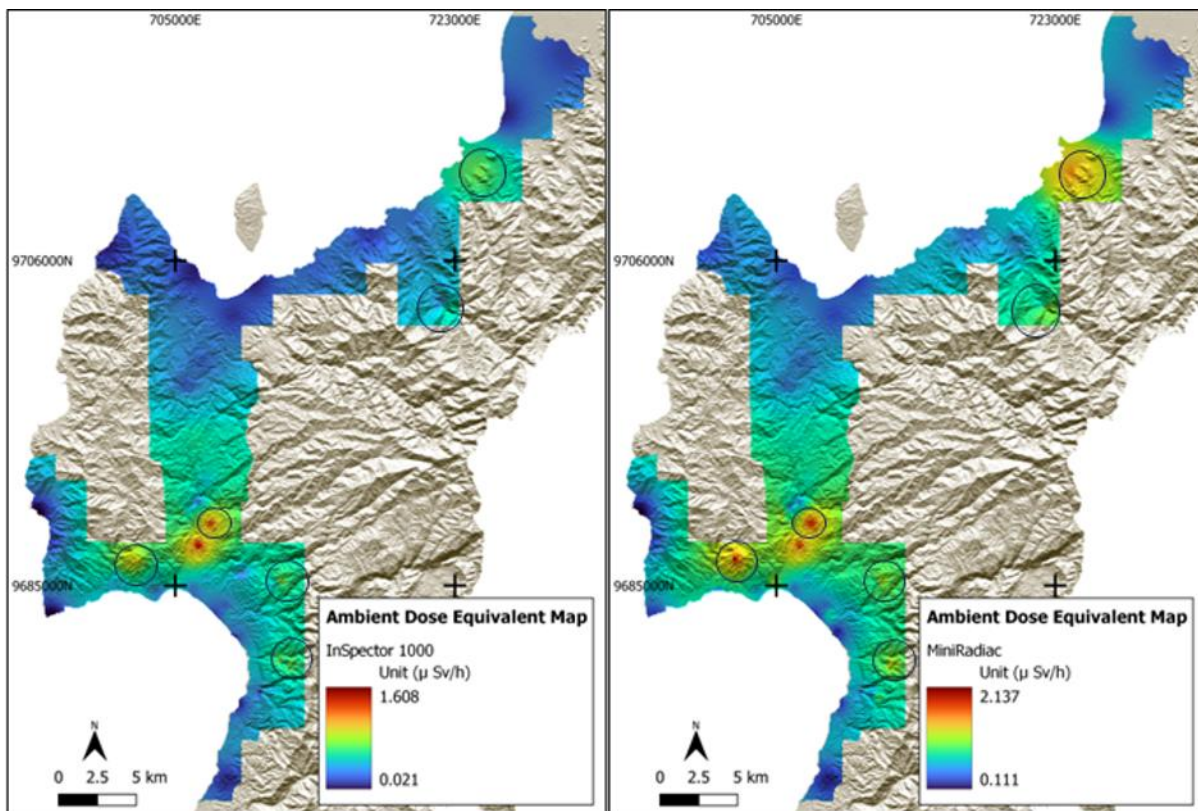


Figure 4 An ambient dose equivalent map, with the left side displaying data collected using the NaI(Tl) scintillator and the right side showing data obtained from the GMC

Saturation is one of the problems faced by instruments in areas with high natural radiation exposure and it can cause readings to exceed the upper limit of the detector (Kakaei et al., 2022; Žunić et al., 2006). Additionally, if gamma or neutron detectors are placed in conditions with high gamma radiation exposure or neutron flux, such as in a nuclear reactor, the count rate calculation must be corrected due to the preamplifier saturation factor (Hashimoto & Yamada, 1999). Unfortunately, in this research evaluating saturation phenomena in the field is not feasible.

In the Hp(10) measurement, we observed an inconsistency where the recorded value was higher than that of H*(10). Hp(10) is defined within the human body (Lips et al., 2021) and its measurement considers the scattering and interaction of radiation, which depend on material composition and geometry. Hp(10) can vary between individuals and locations, and it is influenced by the angle of incidence of incoming radiation (ICRP, 1996). Consequently, the equivalent dose calculated by a personal dosimeter, in cases where radiation exposure comes from all directions, will always be lower than the value measured by a survey meter (MoEG, 2017).

The measurements reveal an unusual condition: the EPD data show higher readings than the survey meter, as illustrated in Figure 2. The discrepancy reaches 54% when compared to NaI(Tl) Scintillator data and 22% with GMC data. The elevated readings from the device are likely due to the type of Geiger-Muller detector used for radiation in one direction only.

EDP, which uses a conventional GM detector, has a relatively flat energy response across a wider energy range, from low to high energy. Meanwhile, the energy-compensated GM is designed to be more selective in responding to energy, with the GMC used in this case only responding to gamma energy. On the other hand, the NaI(Tl) Scintillator detector is more selective in choosing radiation energy, detecting only gamma energy. However, its energy response or efficiency becomes poorer at higher energies (Kadum & Dahmani, 2015). In general, the conventional GM detector used by EPD has a wider energy response range than the energy-compensated GM detector of GMC and the NaI(Tl) Scintillator detector. The specifications of EPD also state that the detector used can detect beta, X-rays, and gamma radiation.

The natural conditions of the research location, which have very high background radiation affect the detector response of each radiation measuring instrument used. The conventional GM detector appears to have a better energy response with a wider energy response range when detecting very high natural radiation exposure. In research locations such as in Mamuju Regency, the radiation sources in the soil are very complex and difficult to determine. One indication of this is the concentration values of U, Th, and K in the surface soil, which are much higher than the world average, as shown in table 2, and the very high average gamma radiation activity values from the nuclides ^{226}Ra , ^{232}Th , and ^{40}K (Rosianna et al., 2020; UNSCEAR, 2010).

We still have a question lingering: does radioactive decay produce X-rays? If so, it's likely that the EPD detects X-rays and has a significant impact on the recorded radiation levels. However, this calls for more investigation. A thorough analysis of the energy spectrum using HPGe Gamma Spectrometer data or other tools like the LaBr Gamma Spectrometer poses a challenge for our future research.

Conclusion

The three radiation measuring instruments used in measuring the natural radiation levels in Mamuju Regency, West Sulawesi, functioned well. The radiation dose rate measurements from these three instruments indicate that Mamuju Regency is categorized as one of the High Natural Background Radiation Areas (HNBRA). Validation of the measurement results with XRF test and HPGe Gamma Spectrometry on 21 soil samples showed a positive correlation through Principal Component Analysis. ^{226}Ra and ^{232}Th are the two main sources of gamma radiation recorded by the survey meters (NaI(Tl) Scintillator and GMC) and the personal dosimeter (EPD), with their correlation visible on the PCA biplot diagram.

Meanwhile, the comparison of the performance of the two survey meters, NaI(Tl) Scintillator and GMC, showed that the GMC detector, with its energy-compensated GM detector specification, has better efficiency when measuring in high radiation areas compared to the NaI(Tl) Scintillator, despite its larger size. The efficiency of the NaI(Tl) Scintillator is known to decrease at high energy, which might be one of the reasons for its lower measurement results compared to the GMC, besides the effects of saturation, which likely disrupt the performance of the NaI(Tl) Scintillator when interacting with high radiation flux.

The higher $H^*(10)$ measured by EPD compared to the measured $H_p(10)$ by NaI(Tl) Scintillator and GMC is mainly due to the difference in detector types. EPD, which uses a conventional GM detector, has a flat and wider energy response with the ability to detect beta, X-ray, and gamma radiation. Meanwhile, the other two instruments only detect gamma radiation, with NaI(Tl) Scintillator known for its poor energy response at high energies. Additionally, the complexity of radiation sources at the research location could also contribute to the measured $H_p(10)$ being higher than $H^*(10)$.

Acknowledgment

The authors would like to acknowledge the Bandung Institute of Technology Research Grant and the Ministry of Research Technology and Higher Education of the Republic of Indonesia for supporting this research activity and publication and The National Research and Innovation Agency (BRIN) of Indonesia for the collaboration and providing all the instruments used during the data acquisition and for the facilities, scientific and technical support from the Environmental Radiation Analysis Laboratory of BRIN in Yogyakarta and Bandung for its collaboration in XRF and HPGe Gamma Spectrometer measurement.

Conflicts of Interest

All authors should disclose in their manuscript any financial or other substantive conflict of interest that might be construed to influence the results or interpretation of their manuscript.

References

Alatas, Z., Hidayati, S., Akhadi, M., Purba, M., Purwadi, D., Ariyanto, S., Winarno, H., Rismiyanto, Sofyatiningrum, Hendriyanto, E., Widyatono, H., Parmanto, E. M., & Syahril. (2016). Buku Pintar Nuklir (Ruslan (ed.); 1st ed.). Batan Press.

ALMisned, G., Zakaly, H. M. H., Ali, F. T., Issa, S. A. M., Ene, A., Kilic, G., Ivanov, V., & Tekin, H. O. (2022). A closer look at the efficiency calibration of LaBr₃(Ce) and NaI(Tl) scintillation detectors using MCNPX for various types of nuclear investigations. *Heliyon*, 8(10), e10839. <https://doi.org/https://doi.org/10.1016/j.heliyon.2022.e10839>

Canberra. (2011). InSpector TM 1000 Digital Hand- Held Multichannel Analyzer. chrome-extension://efaidnbmnnibpcajpcglclefindmkaj/https://www.gammadata.se/assets/Uploads/In1K-SS-C38987.pdf

Casanovas, R., Morant, J. J., & Salvadó, M. (2012). Development and calibration of a real-time airborne radioactivity monitor using gamma-ray spectrometry on a particulate filter. 2012 18th IEEE-NPSS Real Time Conference, 1–4. <https://doi.org/10.1109/RTC.2012.6418383>

Casanovas, R., Prieto, E., & Salvadó, M. (2016). Calculation of the ambient dose equivalent H*(10) from gamma-ray spectra obtained with scintillation detectors. *Applied Radiation and Isotopes*, 118, 154–159. <https://doi.org/https://doi.org/10.1016/j.apradiso.2016.09.001>

Enviro. (n.d.). User Manual Smart Rad Electornic Personal Dosimeter. Available at: <https://fccid.io/OVEEV-IB/User-Manual/User-Manual-1758473>

Godang, S., Idrus, A., Priadi Fadlin, B., & Basuki, N. I. (2019). Saprolitizationâ€TMs Characteristics of Rare Earth Elements in Volcanic Regolith on Drill Core #65 in Western Sulawesi, Indonesia. *Asian Journal of Applied Sciences*, 7(4). <https://doi.org/10.24203/ajas.v7i4.5873>

Hashimoto, K., & Yamada, S. (1999). Counting losses due to saturation effects of scintillation counters at high count rates. *Nuclear Instruments and Methods in Physics Research Section A: Accelerators, Spectrometers, Detectors and Associated Equipment*, 438(2), 502–510. [https://doi.org/10.1016/S0168-9002\(99\)00847-5](https://doi.org/10.1016/S0168-9002(99)00847-5)

Heryana, A. (2023). Bekerja dengan Data Tidak Normal. <https://doi.org/10.13140/RG.2.2.27700.73604>

Hosoda, M., Djatnika, E., Akata, N., Yamada, R., Tamakuma, Y., Sasaki, M., Kelleher, K., Yoshinaga, S., Suzuki, T., & Pornnumpa, C. (2021). A unique high natural background radiation area – Dose assessment and perspectives. *Science of the Total Environment*, 750, 142346. <https://doi.org/10.1016/j.scitotenv.2020.142346>

IAEA. (2003). Guidelines for Radioelement Mapping Using Gamma Ray Spectrometry Data (Issue 1363). International Atomic Energy Agency. <https://www.iaea.org/publications/6746/guidelines-for-radioelement-mapping-using-gamma-ray-spectrometry-data>

ICRP. (1996). Conversion Coefficients for use in Radiological Protection against External Radiation. ICRP Publication 74. *Ann. ICRP* 26 (3-4). Annals of the ICRP, 6, (1). [https://doi.org/10.1016/0146-6453\(81\)90127-5](https://doi.org/10.1016/0146-6453(81)90127-5)

Indrastomo, F. D., Sukadana, I. G., Saepuloh, A., Harsolumakso, A. H., & Kamajati, D. (2015). Interpretation of Mamuju Region Volcanostratigraphy Based on Landsat-8 Image Analysis. *EKSPLORIUM*, 36(2), 71–88. (Text in Indonesian) <https://doi.org/10.17146/Eksplorium.2015.36.2.2772>,

Izewska, J., & Rajan, G. (2005). Radiation dosimeters. IAEA. http://www-pub.iaea.org/MTCD/publications/PDF/Pub1196_web.pdf

Kadum, A., & Dahmani, B. (2015). Efficiency calculation of NaI(Tl) 2 × 2 well-shaped detector. *Instruments and Experimental Techniques*, 58(3), 429–434. <https://doi.org/10.1134/S0020441215030070>

Kakaei, M., Khabazi, H., & Nassiri-Mofakham, N. (2022). A method to overcome the saturation of real-time radon detectors used in high natural radiation regions. *Applied Radiation and Isotopes*, 180, 110025. <https://doi.org/https://doi.org/10.1016/j.apradiso.2021.110025>

Kim, J., Park, K., Hwang, J., Kim, H., Kim, J., Kim, H., Jung, S.-H., Kim, Y., & Cho, G. (2019). Efficient design of a Ø2×2 inch NaI(Tl) scintillation detector coupled with a SiPM in an aquatic environment. *Nuclear Engineering and Technology*, 51(4), 1091–1097. <https://doi.org/https://doi.org/10.1016/j.net.2019.01.017>

Kržanović, N., Stanković, K., Živanović, M., Đaletić, M., & Ciraj-Bjelac, O. (2019). Development and testing of a low cost radiation protection instrument based on an energy compensated Geiger-Müller tube. *Radiation Physics and Chemistry*, 164, 108358. <https://doi.org/https://doi.org/10.1016/j.radphyschem.2019.108358>

Lecoq, P. (2020). Scintillation Detectors for Charged Particles and Photons BT - Particle Physics Reference Library: Volume 2: Detectors for Particles and Radiation (C. W. Fabjan & H. Schopper (eds.); pp. 45–89). Springer International Publishing. https://doi.org/10.1007/978-3-030-35318-6_3

Lehto, J. (2016). BASICS OF NUCLEAR PHYSICS AND OF RADIATION DETECTION AND MEASUREMENT: An open-access textbook for nuclear and radiochemistry students. <https://api.semanticscholar.org/CorpusID:198477191>

Lips, M., Anderson, E., Nishida, K., Schneider, G., Zic, J., Sanders, C., Owen, J., Hondros, J., & de Ruvo, A. (2021). Reflection on the proposed changes to dose quantities-an industrial perspective. *Journal of Radiological Protection : Official Journal of the Society for Radiological Protection*, 41(4). <https://doi.org/10.1088/1361-6498/ac31c3>

LTKMR. (2022a). Calibration Report No. B-294-7/IV / LT / KAUR / 05 / 2022.

LTKMR. (2022b). Calibration Report No . B-294-8 / IV / LT / KAUR / 05 / 2022.

Marques, L., Vale, A., & Vaz, P. (2021). State-of-the-Art Mobile Radiation Detection Systems for Different Scenarios. In *Sensors* (Vol. 21, Issue 4). <https://doi.org/10.3390/s21041051>

Mirion. (2018). UltraRadiacTM-Plus. <https://www.laurussystems.com/wp-content/uploads/7068914D-UltraRadiac-Plus-Users-Manual.pdf>

MoEG, J. (2017). Dose Equivalents: Measurable Operational Quantities for Deriving Effective Doses. BOOKLET to Provide Basic Information Regarding Health Effects of Radiation, Miinistry of the Environment Government Japan. <https://www.env.go.jp/en/chemi/rhm/basic-info/2018/02-03-08.html>

Mouhti, I., Elanique, A., Messous, M. Y., Belhorma, B., & Benahmed, A. (2018). Validation of a NaI(Tl) and LaBr₃(Ce) detector's models via measurements and Monte Carlo simulations. *Journal of Radiation Research and Applied Sciences*, 11(4), 335–339. <https://doi.org/https://doi.org/10.1016/j.jrras.2018.06.003>

Nugraha, E. D., Hosoda, M., Kusdiana, Untara, Mellawati, J., Nurokhim, Tamakuma, Y., Ikram, A., Syaifudin, M., Yamada, R., Akata, N., Sasaki, M., Furukawa, M., Yoshinaga, S., Yamaguchi, M., Miura, T., Kashiwakura, I., & Tokonami, S. (2021). Comprehensive exposure assessments from the viewpoint of health in a unique high natural background radiation area, Mamuju, Indonesia. *Scientific Reports*, 11(1), 14578. <https://doi.org/10.1038/s41598-021-93983-2>

Nugraha, E. D., Hosoda, M., Tamakuma, Y., Kranrod, C., Mellawati, J., Akata, N., & Tokonami, S. (2021). A unique high natural background radiation area in Indonesia: a brief review from the viewpoint of dose assessments. *Journal of Radioanalytical and Nuclear Chemistry*, 330(3), 1437–1444. <https://doi.org/10.1007/s10967-021-07908-4>

NUSTL. (2016). Radiation Dosimeters for Response and Recovery Market Survey Report. In *Radiation Dosimeters for Response and Recovery Market Survey Report* (Issue June). https://www.dhs.gov/sites/default/files/publications/Radiation-Dosimeters-Response-Recovery-MSR_0616-508_0.pdf

Patel, A., & Mazumdar, H. (2023). A review on Radiation Detectors for Various Radiation Detection Applications. *Journal of Radiation and Nuclear Applications*, 8(2), 93–111. <https://doi.org/10.18576/jrna/080201>

Ramadhan, R. A., & Abdullah, K. M.-S. (2018). Background reduction by Cu/Pb shielding and efficiency study of NaI(Tl) detector. *Nuclear Engineering and Technology*, 50(3), 462–469. <https://doi.org/https://doi.org/10.1016/j.net.2017.12.016>

Rosianna, I., Nugraha, E. D., Syaeful, H., Putra, S., Hosoda, M., Akata, N., & Tokonami, S. (2020). Natural Radioactivity of Laterite and Volcanic Rock Sample for Radioactive Mineral Exploration in Mamuju, Indonesia. *Geosciences*, 10(9). <https://doi.org/10.3390/geosciences10090376>

Saindane, S., Pujari, R. N., Murali, S., Narsaiah, M. V. R., Dhole, S. D., & Karmalkar, N. R. (2020). Environmental radiation mapping methodology and applications. <https://doi.org/10.4103/rpe.RPE>

Sukadana, I. G., Harijoko, A., & Setijadji, L. D. (2015). Tectonic Setting of Volcanic Rocks in the Adang Complex, Mamuju Regency, West Sulawesi Province. *Eksplorium: Buletin Pusat Teknologi Bahan Galian Nuklir*, 36(1), 31–44. (Text in Indonesian) <https://doi.org/10.17146/eksplorium.2015.36.1.2769>

Sukadana, I. G., Syaeful, H., Indrastomo, F. D., Widana, K. S., & Rakhma, E. (2016). Identification of Mineralization Type and Specific Radioactive Minerals in Mamuju, West Sulawesi. *Journal of East China University of Technology*, 39, 39–48.

Sukadana, I. G., Warmada, I. W., Harijoko, A., Indrastomo, F. D., & Syaeful, H. (2021). The Application of Geostatistical Analysis on Radiometric Mapping Data to Recognized the Uranium and Thorium Anomaly in West Sulawesi, Indonesia. *IOP Conference Series: Earth and Environmental Science*, 819(1). <https://doi.org/10.1088/1755-1315/819/1/012030>

Syaeful, H., Sukadana, I. G., & Sumaryanto, A. (2014). Radiometric Mapping for Naturally Occurring Radioactive Materials (NORM) Assessment in Mamuju , West Sulawesi. *Atom Indonesia*, 40(1), 33–39. <https://aij.batan.go.id/index.php/aij/article/view/263>

Tavakoli-Anbaran, H., Izadi-Najafabadi, R., & Miri-Hakimabad, H. (2009). The Effect of Detector Dimensions on the NaI (Tl) Detector Response Function. *Journal of Applied Sciences*, 9(11), 5. <https://scialert.net/fulltext/?doi=jas.2009.2168.2173>

Tzortzis, M., & Tsertos, H. (2004). Determination of thorium, uranium and potassium elemental concentrations in surface soils in Cyprus. *Journal of Environmental Radioactivity*, 77(3), 325–338. <https://doi.org/https://doi.org/10.1016/j.jenvrad.2004.03.014>

UNSCEAR. (2000). Sources and effects of ionizing radiation UNSCEAR 2000 report to the General Assembly, with scientific annexes Volume I: Sources. UN. http://inis.iaea.org/search/search.aspx?orig_q=RN:32002971

UNSCEAR. (2010). Sources and Effects of Ionizing Radiation, *UNSCEAR 2008 Report, Volume I: (Sources) Report to the General Assembly, Scientific Annexes A and B (ANNEX B)*: Vol. I. United Nations Publication, New York, USA.

Yavuzkanat, N., Şenyiğit, M., & Kaplan, M. (2022). Investigation of the gamma-ray efficiency for various scintillation detector systems. *Revista Mexicana de Física*, 68(4 Jul-Aug), 041201 1-.
<https://doi.org/10.31349/RevMexFis.68.041201>

Yavuzkanat, N., YalcinN, S., & Gungor, D. (2019). The Determination of the Total Efficiency for NaI(Tl) Detector by GATE Simulation. *BEU Journal of Science*, 8, 37–45. Bitlis Eren University WT - DergiPark.
<https://doi.org/10.17798/bitlisfen.649129>

Zhu, H., Kane, S. C., Croft, S., Venkataraman, R., & Bronson, F. L. (2006). Optimization of the Canberra UltraRadiac GM Tube Wrapping. *2006 IEEE Nuclear Science Symposium Conference Record*, 2, 923–925.
<https://api.semanticscholar.org/CorpusID:2190957>

Žunić, Z. S., Kobal, I., Vaupotić, J., Kozak, K., Mazur, J., Birovljev, A., Janik, M., Čeliković, I., Ujić, P., Demajo, A., Krstić, G., Jakupi, B., Quarto, M., & Bochicchio, F. (2006). High natural radiation exposure in radon spa areas: a detailed field investigation in Niška Banja (Balkan region). *Journal of Environmental Radioactivity*, 89(3), 249–260. <https://doi.org/https://doi.org/10.1016/j.jenvrad.2006.05.010>